

Role of solution chemistry on the trapping of radionuclide Th(IV) using titanate nanotubes as an efficient adsorbent

Guodong Sheng · Baowei Hu

Received: 9 December 2012 / Published online: 4 January 2013
© Akadémiai Kiadó, Budapest, Hungary 2012

Abstract Titanate nanotubes (TNTs) have attracted great interest in multidisciplinary study since their discovery. The adsorption of thorium [Th(IV)] onto TNTs in the absence and presence of humic acid (HA)/fulvic acid (FA) was studied by batch technique. The influence of pH from 2.0 to 10.0, ionic strength from 0.001 to 0.1 mol L⁻¹ NaClO₄, and coexisting electrolyte cations (Li⁺, Na⁺, K⁺) and anions (ClO₄⁻, NO₃⁻, Cl⁻) on the adsorption of Th(IV) onto TNTs was tested. The adsorption isotherms of Th(IV) was determined at pH 3.0 and analyzed with Langmuir and Freundlich adsorption models, respectively. The results demonstrated that the adsorption of Th(IV) onto TNTs increases steeply with increasing pH from 2.0 to 4.0. Generally, HA/FA was showed to enhance Th(IV) adsorption onto TNTs at low pH values, but to reduce Th(IV) adsorption onto TNTs at high pH values. The adsorption of Th(IV) onto TNTs was also dependent on coexisting electrolyte ions in aqueous solution under our experimental conditions. The adsorption of Th(IV) onto TNTs is exothermic and spontaneous. The findings indicating that TNTs can be used as a promising candidate for the enrichment and solidification of Th(IV) or its analogue actinides from large volume solution in real work.

Keywords Thorium(IV) · Titanate nanotubes · Adsorption · Humic acid · Fulvic acid

Introduction

Thoriums have been extensively used in a variety of industrial applications since the last century, and have produced various gaseous, liquid and solid wastes that contain a lot of isotopes of uranium and thorium and their daughter products. Although direct toxicity of thorium is low because of its stability at room temperature, since the liquid wastes of these industrial applications may leak to the surface and can mix with the underground waters, it is increasingly becoming a concerning environmental issue [1]. In addition, tetravalent thorium [Th(IV)] is usually used as an analogue of other tetravalent actinides such as Np(IV) and Pu(IV) in the research of nuclear waste management, which are difficult to be kept in tetravalent form [2–4]. Therefore, the enrichment/separation of Th(IV) through adsorption is an important process in nuclear/radiation chemistry and environmental waste treatment [2–4]. Studies have been carried out to examine different aspects of the adsorption behavior and mechanism of Th(IV) onto oxides and colloids surfaces [1–7].

Since the discovery by Kasuga et al. [8, 9], titanate nanotubes (TNTs) have been used in multidisciplinary areas such as photocatalysis, solar cells, sensors, catalyst supports, ion-exchange materials, electroluminescent hybrid devices and novel adsorbents because of their excellent physico-chemical property [8–12]. Recently, the adsorption behavior of TNTs to different kinds of environmental contaminants including organic dyes [13–16] and radionuclides and/or heavy metal ions [17–20] have been widely studied.

G. Sheng · B. Hu (✉)
School of Life Science and School of Chemistry and Chemical Engineering, Shaoxing University, Huancheng West Road 508, Zhejiang 312000, People's Republic of China
e-mail: hbw@usx.edu.cn

G. Sheng
Key Laboratory of Novel Thin Film Solar Cells, Institute of Plasma Physics, Chinese Academy of Sciences, P.O. Box 1126, Hefei 230031, People's Republic of China

For example, adsorption of organic dyes onto TNTs was studied by Lee and co-workers [14, 15], and it was indicated that the amount of Na(I) within TNT structure was an important factor that dominated the adsorption capacity of organic dyes onto TNTs. Besides, with respect to the adsorption of heavy metal ions onto TNTs, An et al. [19] and Liu et al. [20] found that TNTs showed high adsorption capacity for Cu(II), Pb(II), and Ag(I), and the results revealed that a decrease in adsorption was ascribed to the strengthening O–H bond and the intercalation of H(I) in TNT structure. The adsorption property of Eu(III) and Ni(II) onto TNTs was investigated in previous reports of Sheng et al. [10–12], and it was also found that TNTs showed very high adsorption to Eu(III) and Ni(II). All of these investigations suggested that TNTs are promising adsorbents for the efficient trapping of environmental contaminants in wastewater treatment. However, these limited studies mainly focused on the adsorption kinetic and thermodynamic of organic dyes and heavy metal ions and/or radionuclides onto TNTs and little attention has been paid to the adsorption mechanism of radionuclides onto TNTs [11, 12].

In spite of the extensive studies about the adsorption of organic dyes [13–16] and heavy metal ions and/or radionuclides [17–20] onto TNTs, based on our literature survey, little information about the influence of organic compounds on the adsorption of heavy metal ions and/or radionuclides onto TNTs has been conducted and vice versa. However, it should be pointed out that heavy metal ions and/or radionuclides and organic compounds can be simultaneously existed at many contaminated sites. For example, the existence of humic acid (HA) and fulvic acid (FA) can impose strong influence on the fate and transport of heavy metal ions and/or radionuclides in natural environment. [21–27], thus, the effect of HA/FA on heavy metal ion and/or radionuclide adsorption onto solid particles had been extensively studied in previous reports [21–27]. It was generally found that the adsorption of heavy metal ions and/or radionuclides was increased at low pH values but decreased at high pH values [21–27]. However, the effect of HA/FA on heavy metal ion and/or radionuclide adsorption onto TNTs is still scarce of Sheng et al. [10–12], the effect of HA/FA on Eu(III) and Ni(II) adsorption onto TNTs was studied. Therefore, to better understand the practical application of TNTs as a potential adsorbent in the wastewater management of real work, it is greatly important to investigate the adsorption of heavy metal ions and/or radionuclides onto TNTs in the presence of HA/FA.

Herein, the objectives of this work are to: (1) study the effect of different parameters on Th(IV) adsorption onto TNTs, such as pH, ionic strength, coexisting electrolyte ions, solid content, HA/FA and temperature by using batch techniques (2) determine the thermodynamic parameters of Th(IV) adsorption onto TNTs and (3) presume the adsorption

mechanism of Th(IV) adsorption onto TNTs and to estimate the possible application of TNTs in real wastewater treatment.

Materials and methods

Materials and chemicals

All chemicals used in our experiments were purchased as analytically pure, and no further purification was done. The $\text{Th}(\text{NO}_3)_4$ stock solution was prepared by dissolving ThO_2 in HNO_3 with Milli-Q water under ambient conditions. All other solutions were prepared with Milli-Q water too. HA and FA that carried a large number of O-containing functional groups were extracted from the soil of Hua-Jia County (Gansu province, China) and has been characterized in detail in previous reports [25–28]. The O-containing functional groups of HA and FA had been characterized by fitting the potentiometric titration data as a suite of three discrete acids with pK_a values, and the surface site density of HA and FA were determined to be $6.46 \times 10^{-3} \text{ mol g}^{-1}$ and $2.71 \times 10^{-2} \text{ mol g}^{-1}$, respectively [25–27].

Titanate nanotubes (TNTs) were prepared from TiO_2 particles which is similar to that described by Kasuga et al. [8, 9] by using a simple hydrothermal process. The preparation and characterization of the TNT samples have been described in previous studies [10–12]. Briefly, $\sim 3.0 \text{ g}$ of TiO_2 particles was first mixed with $\sim 90 \text{ mL}$ of 10 mol L^{-1} NaOH solutions, and then, using a simple hydrothermal process, the mixture was treated for $\sim 24 \text{ h}$ at $\sim 150 \text{ }^\circ\text{C}$ in a 250-mL Teflon-lined autoclave. After that, the as-prepared precipitate was washed with $\sim 0.1 \text{ mol L}^{-1}$ HCl solution and Milli-Q water respectively until the rinsing solution pH is close to ~ 7.0 , in the following, the precipitate was separated by a filtration process. The TNT samples were dried at $\sim 120 \text{ }^\circ\text{C}$ for $\sim 8 \text{ h}$ in a vacuum oven and stored in a glass bottle. It can be seen from the scanning electron microscope (SEM) and transmission electron microscopy (TEM) images (Fig. 1) of TNTs, the outer diameter of TNT tube structures is $\sim 10 \text{ nm}$ and the length are 100 nm [11]. It can be determined from the X-ray diffraction (XRD) pattern (Fig. 2a) of the TNT samples that TNTs appears for a scrolled titanate nanosheet ($\text{H}_2\text{Ti}_3\text{O}_7$). The observed peaks ($2\theta \approx 10^\circ, 25^\circ, 29^\circ$ and 50°) in the XRD pattern were assigned to TNTs, and the intense peak at $\sim 10^\circ$ can be attributed to interlayer space of TNTs [11]. From the Fourier transform infrared (FTIR) spectrum (Fig. 2b) of the TNT samples, a broad and intense peak at $\sim 3,200 \text{ cm}^{-1}$ is attributed to the O–H stretching mode, showing the presence of surface hydroxyl groups and water molecules adsorbed on the surface and/or in the interlayer space of TNTs. Water molecules were confirmed by the presence of the peak at $\sim 1,600 \text{ cm}^{-1}$ which is assigned to the H–O–H deformation mode. The peak

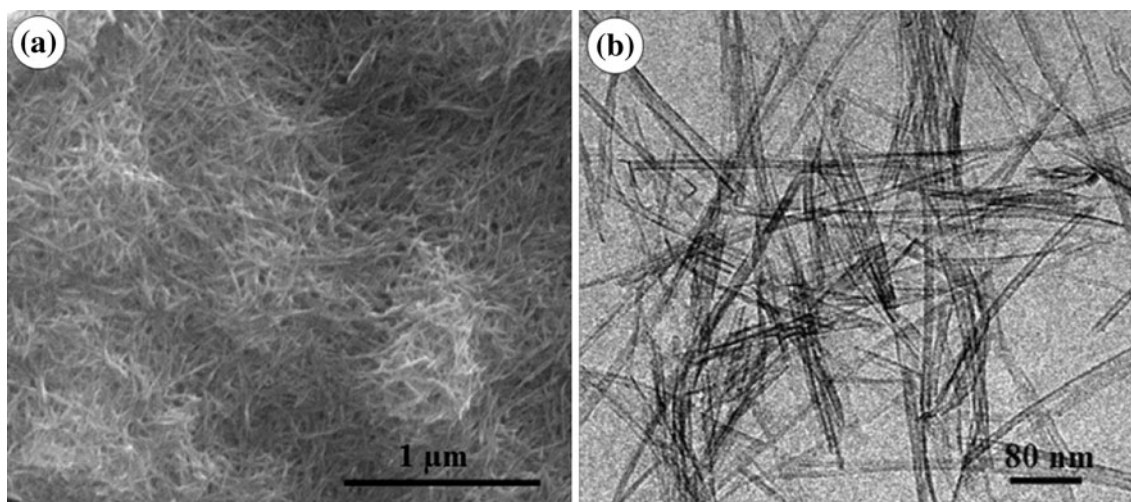


Fig. 1 SEM (a) and TEM (b) images of the TNT samples [11]

observed at $\sim 895\text{ cm}^{-1}$ can be attributed to the Ti–O stretching mode which involves non-bridging oxygen atoms. The peak of $\sim 490\text{ cm}^{-1}$ is attributed to Ti–O–Ti vibrations [11]. The Zeta potentials of the TNT samples as a function of pH are shown in Fig. 3. At $\text{pH} < 4.0$, the TNT samples are positively charged, which is not favorable for metal ion adsorption, while at $\text{pH} > 4.0$, the TNT samples are negatively charged, which is favorable for heavy metal ion and/or radionuclide adsorption [12].

Adsorption experiments

The adsorption of Th(IV) on TNTs was investigated under ambient conditions by using the batch technique in polyethylene centrifuge tubes. In all adsorption experiments, no attempt was made to exclude air. The stock solutions of TNTs and NaClO_4 were pre-equilibrated for $\sim 10\text{ h}$ and then Th(IV) stock solution was added to achieve the desired concentration

of the different components. The system was adjusted to the desired pH by adding negligible amount of $0.01\text{ mol L}^{-1}\text{ HClO}_4$, or $0.01\text{ mol L}^{-1}\text{ NaOH}$. Ionic strengths were adjusted to the desired values with 0.1 or $1.0\text{ mol L}^{-1}\text{ NaClO}_4$ solution. After the suspensions were stirred for $\sim 48\text{ h}$, the solid and liquid phases were separated by centrifugation at $8,000\text{ rpm}$ for 25 min . The concentration of Th(IV) was determined by spectrophotometry at 650 nm using Th(IV)-arsenazo(III) complex. The amount of Th(IV) adsorbed on TNTs was calculated from the difference between initial concentration and equilibrium concentration. The degree of Th(IV) adsorption on test tube walls was determined at $C_0(\text{Th(IV)}) = 20.0\text{ mg L}^{-1}$, $I = 0.01\text{ mol L}^{-1}\text{ NaClO}_4$, $\text{pH} = 3.0$ without TNTs. Results showed that the adsorption of Th(IV) on the test tube walls can be negligible. The adsorption percentage, R , was calculated as follows: $R = (C_0 - C_e) \times 100\% / C_0$, where C_0 (mg L^{-1}) is the initial concentration of Th(IV), and C_e (mg L^{-1}) is the

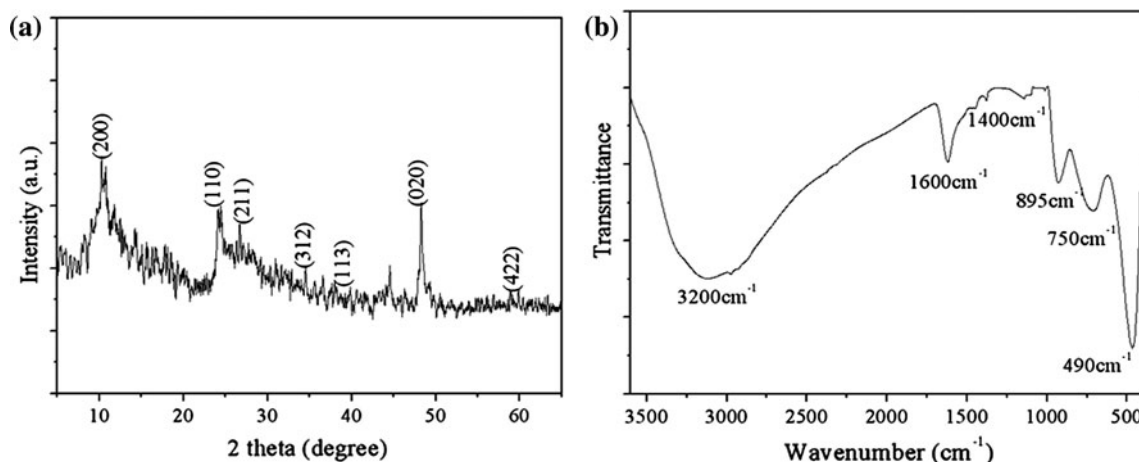


Fig. 2 XRD pattern (a) and FTIR spectrum (b) of the TNT samples [11]

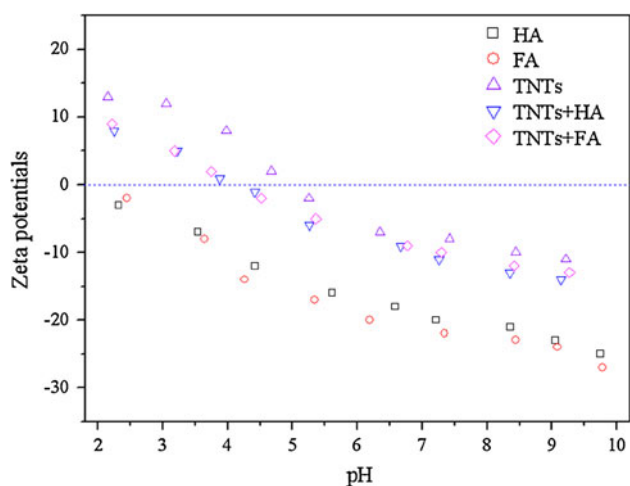


Fig. 3 Zeta potentials of HA, FA, the raw TNT samples and HA/FA coated TNT samples as a function of pH

concentration of Th(IV) in supernatant after adsorption equilibrium. The distribution coefficient, K_d , was calculated from the difference between initial and equilibrium concentration and the concentration of adsorbent dosage: $K_d = \frac{q_e}{C_e} = \frac{C_0 - C_e}{C_e} \cdot \frac{V}{m}$, where q_e (mg g^{-1}) is the concentration of Th(IV) adsorbed on solid phase, V (L) is the volume of the solution, and m (g) is the mass of TNTs in solution.

Results and discussion

Effect of pH and ionic strength

Figure 4 shows the pH dependence of Th(IV) adsorption onto TNTs in a series of NaClO_4 solutions changing from 0.001 to 0.1 mol L^{-1} . It can be clearly seen that the adsorption of Th(IV) onto TNTs is affected by solution pH. The adsorption curve of Th(IV) onto TNTs can be divided into two regions, namely, the adsorption of Th(IV) onto TNTs in 0.001 mol L^{-1} NaClO_4 solution increases gradually from ~ 10 to $\sim 95\%$ with pH increasing from 1.5 to 4.0 (region I), whereas the adsorption of Th(IV) onto TNTs maintains the maximum value of $\sim 95\%$ with pH increasing from pH 4.0 to 9.0 (region II). The results herein are similar to the adsorption of Th(IV) onto MX-80 bentonite [2], $\gamma\text{-Al}_2\text{O}_3$ [3] and anatase [4]. The increase of Th(IV) adsorption onto TNTs with solution pH increasing may be ascribed to the surface properties of TNTs in terms of surface charge and dissociation of surface functional groups of TNTs. The surface of TNTs contains a large number of adsorbing sites and may become positively charged at low pH because of the protonation reaction on TNT surfaces (i.e., $\text{SOH} + \text{H}^+ \rightleftharpoons \text{SOH}_2^+$), thus the electrostatic repulsion occurred between Th(IV) and the positive surface functional

groups (SOH_2^+) onto TNT surface results in the low adsorption efficiency of Th(IV). However, at high pH, TNT surface becomes negatively charged due to deprotonation reaction (i.e., $\text{SOH} \rightleftharpoons \text{SO}^- + \text{H}^+$) and electrostatic repulsion decreases with pH raising because of the reduction of positive charge density on adsorbing sites, which enhances the adsorption of the positively charged Th(IV) through electrostatic attraction. The characteristic of Th(IV) complex that predominates at a specific pH may also play an important role in the removal of TNTs towards Th(IV). According to the hydrolysis constants of Th(IV) in aqueous solutions ($\log \beta_1 = -2.8$, $\log \beta_2 = -7.6$, $\log \beta_3 = -13.1$ and $\log \beta_4 = -8$) [4], the specie distribution of Th(IV) as a function of pH values is shown in Fig. 5. At $\text{pH} < 2.0$, Th^{4+} is the main species ($>80\%$), $\text{Th}(\text{OH})^{3+}$ is less than 14%; at $2.0 < \text{pH} < 4.0$, Th^{4+} and $\text{Th}(\text{OH})^{3+}$ are the main species; at $\text{pH} > 4.0$, $\text{Th}(\text{OH})_4$ is gradually becoming the main species. Therefore, the high adsorption of Th(IV) onto TNTs may be attributed to the precipitation of $\text{Th}(\text{OH})_4$ on the surface of TNTs.

From Fig. 4, it can be also seen that the adsorption of Th(IV) onto TNTs increases with ionic strength decreasing at $\text{pH} < 4.0$. It is well known that ClO_4^- does not form complexes with Th(IV) in aqueous solution and/or on TNTs surfaces. The role of NaClO_4 concentration on Th(IV) adsorption onto TNTs is mainly due to the competition of Na^+ with Th(IV) on TNT surfaces. It can be seen that the adsorption of Th(IV) onto TNTs at $\text{pH} < 4.0$ is obviously affected by ionic strength, whereas no drastic difference of Th(IV) adsorption onto TNTs can be found at $\text{pH} > 4.0$ in the three NaClO_4 solution of different concentrations. The pH- and ionic strength-dependent adsorptions of Th(IV) onto TNTs suggest that the removal of Th(IV) to TNTs is dominated by outer surface complexation and/or

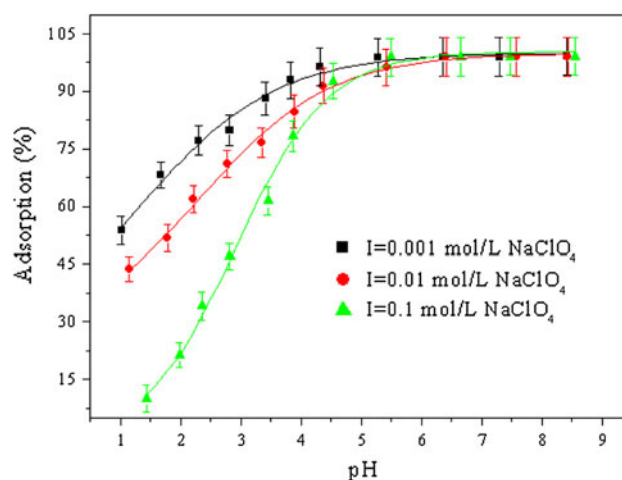


Fig. 4 Effect of ionic strength on Th(IV) adsorption onto TNTs as a function of initial pH, $m/V = 0.5 \text{ g L}^{-1}$, $C_{\text{Th initial}} = 20.0 \text{ mg L}^{-1}$ and $T = 293 \text{ K}$

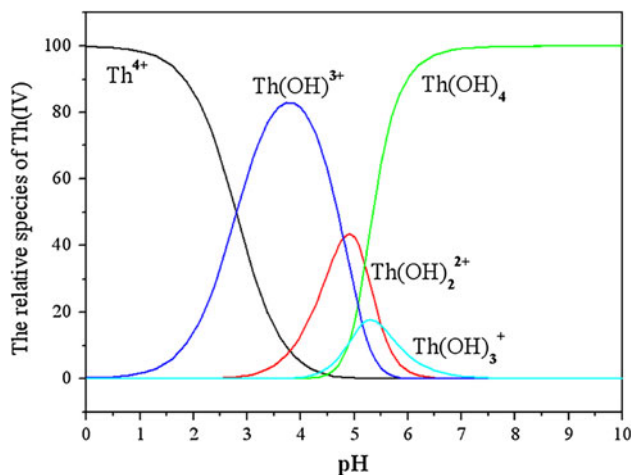


Fig. 5 The relative species of Th(IV) as a function of solution pH

cation exchange at pH < 4.0, whereas the pH- and ionic strength-independent Th(IV) adsorption onto TNTs indicates that the adsorption of Th(IV) onto TNTs is mainly due to inner surface complexation and/or surface precipitation at pH > 4.0 studied herein [29].

Effects

From Fig. 6, one can see that HA/FA strongly affects the adsorption of Th(IV) onto TNTs, showing the adsorption of Th(IV) onto TNTs is obviously enhanced at low pH values (i.e., from 2.0 to 4.0), but is reduced at high pH values (i.e., at pH > 4.0). In the presence of HA/FA, (HA/FA)-Th complexes can be formed. At low pH values, these Th complexes can be easily adsorbed onto TNT surface, leading to the enhanced adsorption of Th(IV) onto TNTs. Additionally, the adsorbed HA/FA may introduce more

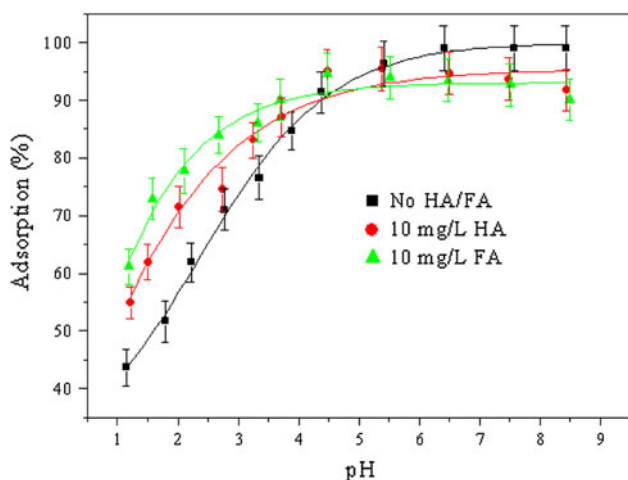


Fig. 6 Effect of HA/FA on the adsorption of Th(IV) onto TNTs as a function of initial pH, $I = 0.01 \text{ mol L}^{-1} \text{ NaClO}_4$, $m/V = 0.5 \text{ g L}^{-1}$, $C_{\text{Th(IV)initial}} = 20.0 \text{ mg L}^{-1}$ and $T = 293 \text{ K}$

negative surface charge on the surface of TNTs, allowing more Th(IV) to be adsorbed onto TNT surface due to favorable electrostatic interaction. At high pH values, the negatively charged HA/FA is weakly adsorbed onto TNT surfaces and the stable complex (HA/FA)-Th can be easily dissolved in aqueous solution, leading to the decreased adsorption of Th(IV) onto TNTs. Herein, we determined the zeta potentials (Fig. 3) of HA and FA, and HA/FA coated TNTs as a function of pH, respectively, and it can be found from Fig. 3 that both FA and HA have negative ζ potentials at pH > 2.0. Therefore, at low pH values, the negatively charged HA/FA can be easily adsorbed on the positively charged surfaces of TNTs (Fig. 7) due to electrostatic attraction, while the negatively charged FA/HA can be hardly adsorbed on the negatively charged surfaces of TNTs (Fig. 7) due to electrostatic repulsion at high pH values. Due to the adsorption of HA/FA onto TNTs, the values of ζ potentials of HA/FA coated TNTs are less positive at low pH values, while more negative at high pH values, compared to those of bare TNTs (Fig. 3). Based on these analysis, the strong complexation ability of surface adsorbed HA/FA with Th(IV) should enhance the adsorption of Th(IV) onto TNTs. The complexation between Th(IV) and HA/FA is more stronger than that between Th(IV) and TNTs. However, with solution pH increasing, the negatively charged HA/FA can be difficultly adsorbed on the negatively charged TNTs surface due to electrostatic repulsion. At high pH values, The competition between soluble HA/FA and TNTs with Th(IV) increases the formation of strong HA/FA-Th complexes in solution, thereby competitively diminishing the extent of Th(IV) adsorption on HA/FA-TNTs hybrids [2, 3].

One can also see from Fig. 6 that the effect of FA on Th(IV) adsorption onto TNTs is much stronger than the

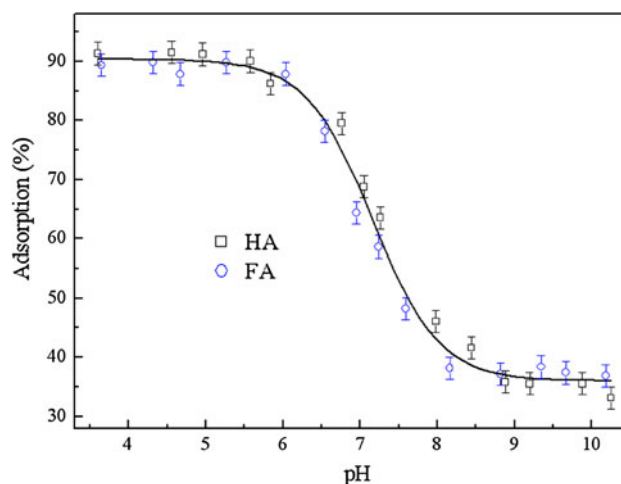


Fig. 7 Adsorption of HA and FA onto TNTs as a function of pH, $C_{\text{(HA/FA)}} = 10.0 \text{ mg L}^{-1}$, $m/V = 0.5 \text{ g L}^{-1}$, $I = 0.01 \text{ mol L}^{-1} \text{ NaClO}_4$, $T = 20 \text{ }^\circ\text{C}$ [11]

effect of HA on Th(IV) adsorption onto TNTs at the whole pH range at the same concentrations. Although HA and FA were extracted from the same soil sample and both of HA and FA contain similar O-containing functional groups such as carboxyl ($-\text{COOH}$), hydroxyl ($-\text{OH}$) and phenolic ($-\text{Ph}-\text{OH}$) groups, the proportions and configurations of these O-containing functional groups are quite different. The surface site density of FA (i.e., $2.71 \times 10^{-2} \text{ mol g}^{-1}$) is higher than that of HA (i.e., $6.46 \times 10^{-3} \text{ mol g}^{-1}$), suggesting that FA can provide more available adsorbing sites for the adsorption Th(IV) onto TNTs [22–25]. So it is quite reasonable that FA has a stronger effect on Th(IV) adsorption onto TNTs than HA does. In previous investigations, Xu et al. [2] studied the effect of HA/FA on Th(IV) adsorption onto MX-80 bentonite, Chen et al. [3] studied the effect of HA/FA on Th(IV) adsorption onto $\gamma\text{-Al}_2\text{O}_3$, Tan et al. [4] studied the influence of HA/FA on Th(IV) adsorption onto anatase, and similar findings have been reported.

Effect of coexisting electrolyte ions

Figure 8 shows that the adsorption of Th(IV) from aqueous solution onto TNTs was clearly affected by different coexisting electrolyte ions, i.e., Na^+ , K^+ , Li^+ , ClO_4^- , NO_3^- and Cl^- , respectively. From Fig. 8a, the adsorption of Th(IV) onto TNTs is strongly affected by coexisting electrolyte cations. The adsorption of Th(IV) onto TNTs at pH 1.0–4.0 are in the following sequence: $\text{K}^+ < \text{Na}^+ < \text{Li}^+$, showing that coexisting electrolyte cations can affect the adsorption of Th(IV) onto TNT surfaces. The coexisting electrolyte cations in solution will compete for interaction with the surface of TNTs, and Th(IV) have higher charge and higher affinity to the surface of TNTs than the alkali metals. As support for this competition principle, the order of TNTs uptake at pH 1.0–4.0 was found to be the highest for Li^+ and the lowest for K^+ , which is the order of their radii of hydration: $\text{K}^+ = 2.32$, $\text{Na}^+ = 2.76$ and $\text{Li}^+ = 3.4 \text{ \AA}$ [3]. The adsorption of Th(IV) onto TNTs can be considered as a competition of Th(IV) with Li^+ (or Na^+ , K^+) at TNT surfaces. The radius of Li^+ is larger than those of the other two cations and therefore the effect of Li^+ on Th(IV) adsorption onto TNTs is smaller than those of Na^+ and K^+ . From Fig. 8b, it can be seen that the order of decrease in the adsorption of Th(IV) onto TNTs is the highest in NaClO_4 solution and the lowest in NaCl solution at pH < 4.0. The following reasons can be used to explain this phenomenon: (1) Idiocratic adsorption of Cl^- onto the surfaces of TNTs is a little easier than that of NO_3^- and ClO_4^- , and thus Cl^- adsorption on the surfaces of TNTs changes the surface properties of TNTs and decreases the availability of adsorbing sites for the adsorption of Th(IV); (2) Cl^- and NO_3^- can form soluble complexes with Th(IV) in aqueous solution, while ClO_4^- can be not formed

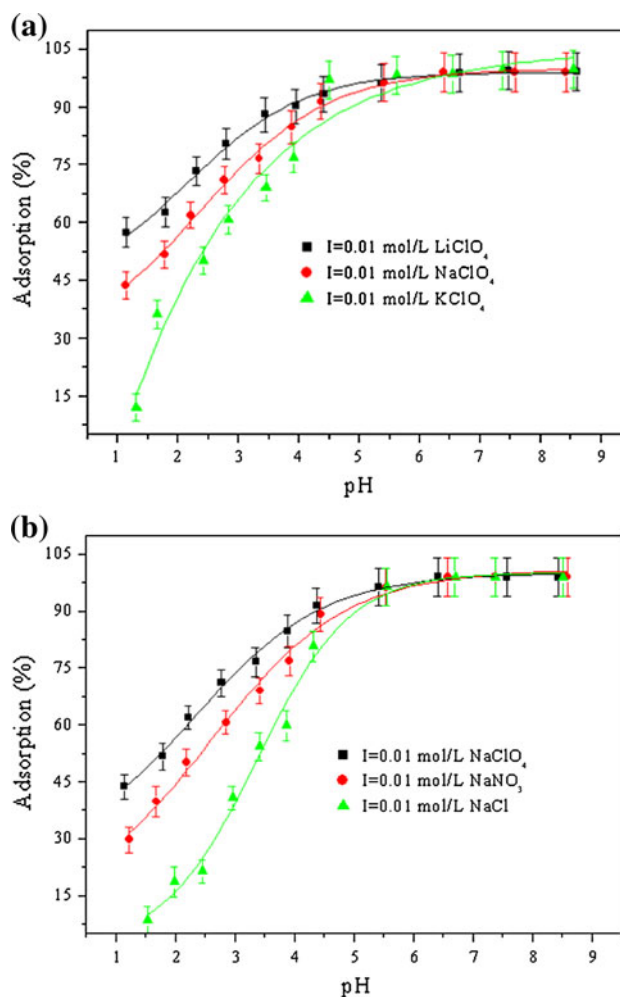


Fig. 8 Effect of coexisting electrolyte cation (a) and anion (b) ions on the adsorption of Th(IV) onto TNTs as a function of initial pH, $m/V = 0.5 \text{ g L}^{-1}$, $C_{\text{Th(IV)initial}} = 20.0 \text{ mg L}^{-1}$ and $T = 293 \text{ K}$

soluble complexes with Th(IV) in aqueous solution. (3) The radicals radium sequence is $\text{Cl}^- < \text{NO}_3^- < \text{ClO}_4^-$, the smaller radium radicals can take up more adsorbing sites and contribute to the decrease of Th(IV) adsorption onto TNTs [2, 29].

Effect of adsorbent content

The effect of adsorbent content on the adsorption of Th(IV) from aqueous solution onto TNTs is shown in Fig. 9. It can be clearly found that the extent of adsorption percentage (%) of Th(IV) onto TNTs increases with solid content increasing (Fig. 9a). This is to be expected because, for a fixed initial Th(IV) concentration, increasing TNT content can provide more adsorption sites and thereby increases the adsorption of Th(IV) onto TNTs [30]. However, the concentration of Th(IV) adsorbed on TNTs decreases with TNT content increasing (Fig. 9b). This phenomena can be attributed to the following factors: (1) a higher amount of

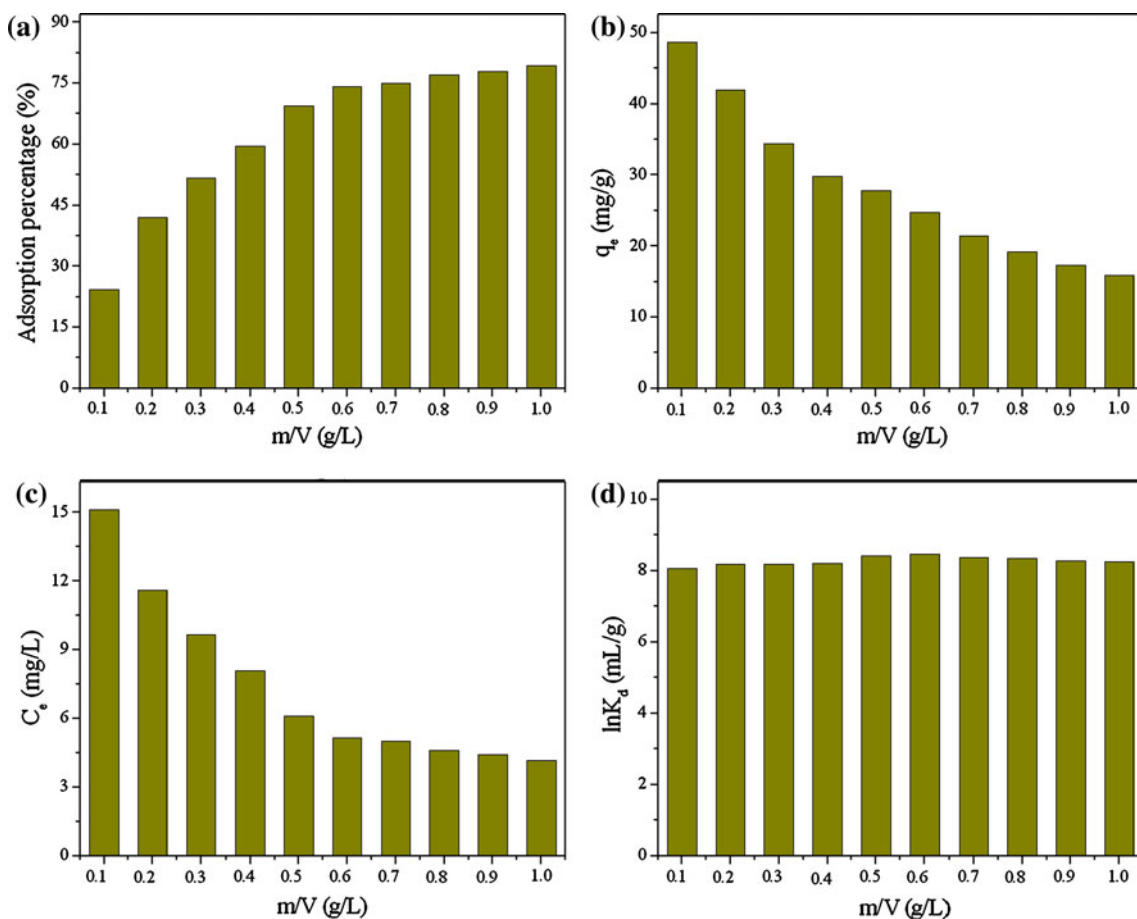


Fig. 9 Adsorption of Th(IV) onto TNTs as a function of solid content, pH = 3.0, I = 0.01 mol L⁻¹ NaClO₄, m/V = 0.5 g L⁻¹, C_{(Th)initial} = 20.0 mg L⁻¹ and T = 293 K

TNT effectively reduces the unsaturation of adsorption sites, and thus the number of such sites per unit mass comes down resulting in comparatively less adsorption at higher TNT amount; (2) when TNT content is low, the Th(IV) can easily access the adsorption sites and thus results the high values of adsorption capacity. With the increase in TNT content, the corresponding increase in adsorption per unit mass of TNTs is less because of lower adsorption capacity utilization of TNTs, which may be ascribed to overcrowding of TNT particles that may be termed as a kind of solid concentration effect; (3) higher TNT content can create particle aggregation, thus resulting in the decrease of the total surface area and the increase in diffusional path length, contributing to the decrease in adsorption capacity [31, 32]. From Fig. 9c, it is clear that the final concentration of Th(IV) remained in solution and the concentration of Th(IV) adsorbed on TNTs both decrease with TNT content increasing. This is certainly a capacity effect [33, 34]. However, the distribution coefficient does not change with TNT content increasing (Fig. 9d), which is consistent to the physicochemical properties of the values of distribution coefficient (i.e., the value of distribution

coefficient is independent of solid content at low solid concentrations) [34, 35].

Adsorption isotherms and thermodynamics

The adsorption isotherms for Th(IV) adsorbed onto TNTs at 293, 313 and 333 K are shown in Fig. 10. The adsorption isotherm is the highest at T = 333 K and is the lowest at T = 293 K. The result indicates that high temperature is advantageous for Th(IV) adsorption onto TNTs. The Langmuir and Freundlich isotherm models are used to simulate the adsorption isotherms of Th(IV) adsorption onto TNTs and to establish the relationship between the amount of Th(IV) adsorbed onto TNTs and the concentration of Th(IV) remained in aqueous solution. The Langmuir model assumes that adsorption of Th(IV) onto TNTs occurs in a monolayer with all adsorption sites identical and energetically equivalent [34–36]. The form of the Langmuir model can be described by the following equation: $q_e = \frac{bq_{\text{Max}}C_e}{1+bC_e}$, which can be expressed in linear form: $\frac{1}{q_e} = \frac{1}{q_{\text{Max}}} + \frac{1}{bq_{\text{Max}}} \cdot \frac{1}{C_e}$, where C_e is the equilibrium concentration of Th(IV) remained in aqueous solution

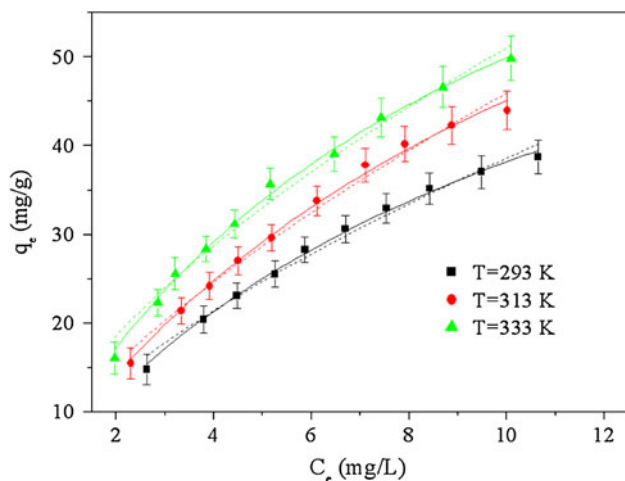


Fig. 10 Adsorption isotherm, Langmuir and Freundlich model fitting for Th(IV) adsorption onto TNTs at three different temperatures, pH = 3.0, I = 0.01 mol L⁻¹ NaClO₄, m/V = 0.5 g L⁻¹, initial Th(IV) concentration = 10–40 mg L⁻¹, symbols denote experimental data, solid lines represent the model fitting of Langmuir equation, dash lines represent the model fitting of Freundlich equation

(mg L⁻¹); q_e is the amount of Th(IV) adsorbed on per weight unit of TNTs after equilibrium (mg g⁻¹); q_{\max} , the maximum adsorption capacity of Th(IV) onto TNTs, is the amount of Th(IV) at complete monolayer coverage (mg g⁻¹), and b (L mol⁻¹g) is a constant that relates to the heat of adsorption of Th(IV) onto TNTs. The Freundlich isotherm model allows for several kinds of adsorption sites on TNT surface and represents properly the adsorption data at low and intermediate concentrations on heterogeneous surfaces [34–36]. The equation of the Freundlich model is represented by the equation: $q_e = k_F C_e^n$, which can be expressed in linear form: $\log q_e = \log k_F + n \log C_e$, where k_F (mg¹⁻ⁿ g⁻¹ Lⁿ) represents the adsorption capacity of Th(IV) onto TNTs when Th(IV) equilibrium concentration equals to 1, and n represents the degree of dependence of adsorption of Th(IV) onto TNTs with equilibrium concentration [34–36]. The relative values calculated from the Langmuir and Freundlich isotherm models are listed in Table 1. From Fig. 10 and the R^2 values of Table 1, we can see that the Langmuir model fits the experimental data of Th(IV) adsorption onto TNTs better than the

Freundlich model, suggesting that the binding energy on the whole surface of TNTs is uniform. The values of q_{\max} obtained from the Langmuir model for Th(IV) adsorption onto TNTs are the highest at T = 333 K and the lowest at T = 293 K, indicating that the adsorption of Th(IV) onto TNTs is improved with reaction temperature increasing.

The thermodynamic parameters (ΔH° , ΔS° , and ΔG°) for Th(IV) adsorption onto TNTs can be determined from the temperature-dependent adsorption. Free energy change (ΔG°) is calculated from the relationship: $\Delta G^\circ = -RT \ln K^\circ$, where K° is the adsorption equilibrium constant of Th(IV) onto TNTs. Values of $\ln K^\circ$ obtained by plotting $\ln K_d$ versus q_e for the adsorption of Th(IV) onto TNTs (Fig. 11) and extrapolating q_e to zero [28, 34–36] are 8.79 (T = 293 K), 8.94 (T = 313 K) and 9.15 (T = 333 K) (Table 2), respectively. Standard entropy change (ΔS°) is calculated using the equation: $\left(\frac{\partial \Delta G^\circ}{\partial T}\right)_P = -\Delta S^\circ$. The average standard enthalpy change (ΔH°) is then calculated from the expression: $\Delta H^\circ = \Delta G^\circ + T\Delta S^\circ$. The values obtained from these equations are tabulated in Table 3. A positive value of the standard enthalpy change (ΔH°) shows that the adsorption of Th(IV) onto TNTs is endothermic. One possible explanation to this positive entropy is that Th(IV) is solved well in water, and the hydration sheath of Th(IV) has to be destroyed before its adsorption onto TNTs. This dehydration process needs energy, and it is favored at high temperature. The removal of water from ions is essentially an endothermic process, and it appears that the endothermicity of the desolvation process exceeds that of the enthalpy of adsorption by a considerable extent [23, 27, 35]. As is expected for a spontaneous process under the experimental conditions, it is clear that the free energy changes (ΔG°) of Th(IV) adsorption onto TNTs is more negative at higher temperature, which indicates that the spontaneity of the adsorption process increases with the rise in temperature. The positive value of entropy change (ΔS°) implies some structural changes in sorbate and sorbent during the adsorption process, which leads to an increase in the disorderness of the solid-solution system [23, 27]. The thermodynamic analysis derived from temperature-dependent adsorption isotherms shows that the adsorption of Th(IV) onto TNTs is spontaneous and endothermic.

Table 1 The parameters for Langmuir and Freundlich adsorption isotherms of Th(IV) onto TNTs at different temperatures

| T (K) | Langmuir | | | Freundlich | | |
|-------|----------------------------------|----------------------------|-------|---|-------|-------|
| | q_{\max} (mg g ⁻¹) | b (L mol ⁻¹) | R | K_F (mg ¹⁻ⁿ L ⁿ g ⁻¹) | n | R |
| 293 | 50.97 | 0.089 | 0.995 | 8.72 | 0.645 | 0.987 |
| 313 | 69.76 | 0.082 | 0.996 | 9.59 | 0.680 | 0.988 |
| 333 | 95.24 | 0.110 | 0.996 | 11.99 | 0.629 | 0.987 |

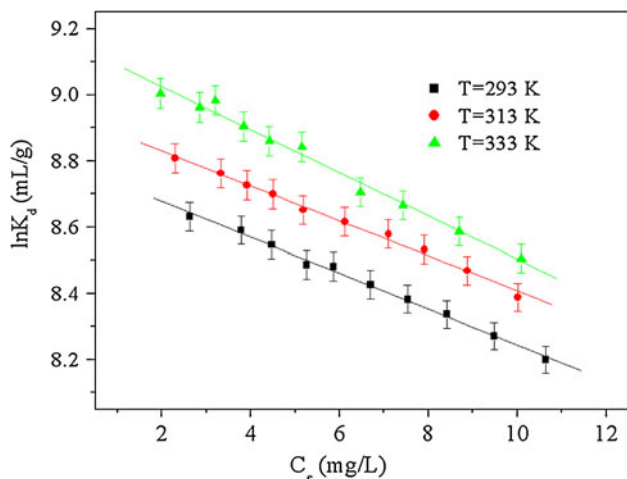


Fig. 11 The linear fit of $\ln K_d$ versus q_e ($\ln K_d = A + Bq_e$) for Th(IV) adsorption on TNTs, pH = 3.0, I = 0.01 mol L⁻¹ NaClO₄, m/V = 0.5 g L⁻¹, initial Th(IV) concentration = 10–40 mg L⁻¹

Table 2 Constants of linear fit of $\ln K_d$ versus q_e ($\ln K_d = A + Bq_e$) for Th(IV) adsorption onto TNTs

| T (K) | A | B | R |
|-------|------|--------|-------|
| 293 | 8.79 | -0.054 | 0.995 |
| 313 | 8.94 | -0.053 | 0.993 |
| 333 | 9.15 | -0.065 | 0.988 |

Table 3 Values of thermodynamic parameters for the adsorption of Th(IV) onto TNTs

| T (K) | ΔG° (kJ mol ⁻¹) | ΔH° (kJ mol ⁻¹) | ΔS° (J mol ⁻¹ K ⁻¹) |
|-------|--|--|---|
| 293 | -21.41 | 35.98 | 195.9 |
| 313 | -23.26 | 38.05 | 195.9 |
| 333 | -25.33 | 39.91 | 195.9 |

Conclusion

In the light of the finding of this work, the following main conclusions can be stressed: The adsorption capacity of Th(IV) onto TNTs is very high. The Langmuir isotherm model described the data better than the Freundlich model. Langmuir model fitted the adsorption data of Th(IV) onto TNTs better than the Freundlich model. The adsorption of Th(IV) onto TNTs was also dependent on HA/FA and coexisting electrolyte ions in aqueous solution under our experimental conditions. The adsorption of Th(IV) onto TNTs is exothermic and spontaneous. Therefore, TNTs exhibit promising application in the field of nuclear science and technology for the enrichment and solidification of radionuclides.

Acknowledgments Financial supports from department of science and technology, Zhejiang province (2010C33101), the science and technology program of Shaoxing (2011A23006) and the National Natural Science Foundation of China (21207092; 20907055; 20971126) are acknowledged.

References

1. Talip Z, Eral M, Hiçsonmez U (2009) Adsorption of thorium from aqueous solutions by perlite. *J Environ Radioact* 100: 139–143
2. Xu D, Wang XK, Chen CL, Zhou X, Tan XL (2006) Influence of soil humic acid and fulvic acid on sorption of thorium(IV) on MX-80 bentonite. *Radiochim Acta* 94:429–434
3. Chen C, Wang X (2007) Influence of pH, soil humic/fulvic acid, ionic strength and foreign ions on sorption of thorium(IV) onto γ -Al₂O₃. *Appl Geochem* 22:436–445
4. Tan X, Wang X, Fang M, Chen C (2007) Sorption and desorption of Th(IV) on nanoparticles of anatase studied by batch and spectroscopy methods. *Colloids Surf A* 296:109–116
5. Guerra DL, Vian RR, Airoldi C (2009) Adsorption of thorium cation on modified clays MTTZ derivative. *J Hazard Mater* 168: 1504–1511
6. Reiller P, Casanova F, Molin V (2005) Influence of addition order and contact time on thorium(IV) retention by hematite in the presence of humic acids. *Environ Sci Technol* 39:1641–1648
7. Rojo I, Seco F, Rovira M, Giménez J, Cervantes G, Martí V, de Pablo J (2009) Thorium sorption onto magnetite and ferrihydrite in acidic conditions. *J Nucl Mater* 385:474–478
8. Kasuga T, Hiramatsu M, Hoson A, Sekino T, Niihara K (1998) Formation of titanium oxide nanotube. *Langmuir* 14:3160–3163
9. Kasuga T, Hiramatsu M, Hoson A, Sekino T, Niihara K (1999) Titania nanotubes prepared by chemical processing. *Adv Mater* 11:1307–1311
10. Sheng G, Yang S, Sheng J, Zhao D, Wang X (2011) Influence of solution chemistry on the removal of Ni(II) from aqueous solution to titanate nanotubes. *Chem Eng J* 168:178–182
11. Sheng G, Yang S, Zhao D, Sheng J, Wang X (2012) Adsorption of Eu(III) on titanate nanotubes studied by a combination of batch and EXAFS technique. *Sci China Chem* 55:182–194
12. Sheng G, Dong H, Shen R, Li Y Microscopic insights into the temperature-dependent adsorption of Eu(III) onto titanate nanotubes studied by FTIR, XPS, XAFS and batch technique, *Chem Eng J*. doi: 10.1016/j.cej.2012.10.076
13. Bavykin DV, Redmond KE, Nias BP, Kulak AN, Walsh FC (2010) The effect of ionic charge on the adsorption of organic dyes onto titanate nanotubes. *Aust J Chem* 63:270–275
14. Lee CK, Lin KS, Wu CF, Lyu MD, Lo CC (2008) Effects of synthesis temperature on the microstructures and basic dyes adsorption of titanate nanotubes. *J Hazard Mater* 150:494–503
15. Lee CK, Wang CC, Juang LC, Lyu MD, Hung SH, Liu SS (2008) Effects of sodium content on the microstructures and basic dye cation exchange of titanate nanotubes. *Colloids Surf A* 317: 164–173
16. Xiong L, Yang Y, Mai JX, Sun WL, Zhang CY, Wei DP, Chen Q, Ni JR (2010) Adsorption behavior of methylene blue onto titanate nanotubes. *Chem Eng J* 156:313–320
17. Niu HY, Wang JM, Shi YL, Cai YQ, Wei FS (2009) Adsorption behavior of arsenic onto protonated titanate nanotubes prepared via hydrothermal method. *Micro Macro Mater* 122:28–35
18. Chen YC, Lo SL, Kuo J (2010) Pb(II) adsorption capacity and behavior of titanate nanotubes made by microwave hydrothermal method. *Colloids Surf A* 361:126–131

19. An HQ, Zhu BL, Wu HY, Zhang M, Wang SR, Zhang SM, Wu SH, Huang WP (2008) Synthesis and characterization of titanate and CS₂-modified titanate nanotubes as well as their adsorption capacities for heavy metal ions. *Chem J Chin U* 29:439–444
20. Liu SS, Lee CK, Chen HC, Wang CC, Juang LC (2009) Application of titanate nanotubes for Cu(II) ions adsorptive removal from aqueous solution. *Chem Eng J* 147:188–193
21. Sheng G, Li Y, Dong H, Shao D (2012) Environmental condition effects on radionuclide ⁶⁴Cu(II) sequestration to a novel composite: polyaniline grafted multiwalled carbon nanotubes. *J Radioanal Nucl Chem* 293:797–806
22. Hu B, Cheng W, Zhang H, Sheng G (2010) Sorption of radionickel to goethite: effect of water quality parameters and temperature. *J Radioanal Nucl Chem* 285:389–398
23. Hu BW, Cheng W, Zhang H, Yang ST (2010) Solution chemistry effects on sorption behavior of radionuclide ⁶³Ni(II) in illite-water suspensions. *J Nucl Mater* 406:263–270
24. Sheng G, Dong H, Li Y (2012) Characterization of diatomite and its application for the retention of radiocobalt: role of environmental parameters. *J Environ Radioact* 113:108–115
25. Sheng G, Shen R, Dong H, Li Y Colloidal diatomite, radionickel and humic substance interaction: A combined batch, XPS and EXAFS investigation, *Environ Sci Pollut Res*. doi: [10.1007/s11356-012-1278-1](https://doi.org/10.1007/s11356-012-1278-1)
26. Tan XL, Wang XK, Geckeis H, Rabung Th (2008) Sorption of Eu(III) on humic acid or fulvic acid bound to hydrous alumina studied by SEM-EDS, XPS, TRLFS and batch techniques. *Environ Sci Technol* 42:6532–6537
27. Yang S, Sheng G, Tan X, Hu J, Du J, Montavon G, Wang X (2011) Determination of Ni(II) uptake mechanisms on mordenite surfaces: A combined macroscopic and microscopic approach. *Geochim Cosmochim Acta* 75:6520–6534
28. Sheng G, Li Y, Yang X, Ren X, Yang S, Hu J, Wang X Efficient removal of arsenate by a versatile magnetic graphene oxide composites, *RSC Adv*. doi: [10.1039/c2ra21623j](https://doi.org/10.1039/c2ra21623j)
29. Sheng G, Hu J, Wang X (2008) Sorption properties of Th(IV) on the raw diatomite-effects of contact time, pH, ionic strength and temperature. *Appl Radiat Isot* 66:1313–1320
30. Rengaraj S, Yeon KH, Kang SY, Lee JU, Kim KW, Moon SH (2002) Studies on adsorptive removal of Co(II), Cr(III) and Ni(II) by IRN77 cation-exchange resin. *J Hazard Mater B* 92:185–198
31. Shukla A, Zhang YH, Dubey P, Margrave JL, Shukla SS (2002) The role of sawdust in the removal of unwanted materials from water. *J Hazard Mater B* 95:137–152
32. Bhattacharyya KG, Gupta SS (2008) Adsorption of Fe(III), Co(II) and Ni(II) on ZrO-kaolinite and ZrO-montmorillonite surfaces in aqueous medium. *Colloids Surf A* 317:71–79
33. Yu B, Zhang Y, Shukla A, Shukla SS, Dorris KL (2000) The removal of heavy metal from aqueous solutions by sawdust adsorption-removal of copper. *J Hazard Mater B* 80:33–42
34. Sheng G, Hu J, Jin H, Yang S, Ren X, Li J, Chen Y, Wang X (2010) Effect of humic acid, fulvic acid, pH, ionic strength and temperature on ⁶³Ni(II) sorption to MnO₂. *Radiochim Acta* 98:291–299
35. Chen CL, Wang XK (2006) Adsorption of Ni(II) from aqueous solution using oxidized multiwall carbon nanotubes. *Ind Eng Chem Res* 45:9144–9150
36. Yang S, Guo Z, Sheng G, Wang X (2012) Investigation of the sequestration mechanisms of Cd(II) and 1-naphthol on discharged multi-walled carbon nanotubes in aqueous environment. *Sci Total Environ* 420:214–221